

# PV SELF-CONSUMPTION DERIVED FROM HIGHLY GRANULAR FIELD DATA AND THE INFLUENCE OF TEMPORAL RESOLUTION

*Christoph Stegner<sup>1\*</sup>*

ZAE Bayern, Hof, Germany  
\*christoph.stegner@zae-bayern.de

**Keywords:** PV SELF-CONSUMPTION, LOAD PROFILES, TEMPORAL RESOLUTION, SAMPLING RATE, SENSITIVITY ANALYSIS

## Abstract

Thanks to its high scalability, photovoltaics can be employed across various use cases. The primary motivation is often local self-consumption. Therefore, defining characteristic metrics is crucial, which are discussed in detail in this study, including underlying mathematics. Then the size of the PV system, the most significant influencing factor, is analysed, in terms of the energy generated to load ratio. While the sizing of the PV system is intended to provide a degree of freedom, there is a parameter that can involuntarily falsify the calculation of self-consumption: the temporal resolution of the time series used. Therefore, a sensitivity analysis is carried out to evaluate the extent of its impact. The author employs measurement data of unparalleled granularity, matching various loads with PV systems by simulation. The loads extend beyond the residential sector including a fast-food takeaway and a mixed commercial site. The latter, with its significantly higher electricity consumption, challenges the commonly held belief in the literature that the time resolution of the PV profile is always of secondary importance. Due to the high temporal resolution of some of the measurements of one second, reliable recommendations are made regarding minimum sampling rates.

## 1. Introduction

No other technology for generating electrical energy can be scaled as well as photovoltaics (PV). As a result, even small systems with just a few kW<sub>p</sub> can be implemented economically and safely. This has led to the installation of millions of PV systems, providing power where it is required. For the user, reaching a high degree of self-consumption of the electricity generated is generally the primary motivation. But a comprehensive grasp of this crucial metric is also essential for grid operators because any surplus electricity can be supplied to the grid when necessary. In many countries, including Germany, it is even mandatory for grid operators to do so.

The level of self-consumption is determined by the synchronicity of generation and load. Due to the high volatility of the corresponding time series, the accuracy of the matching has a considerable impact on the outcome. This accuracy is defined by the temporal resolution of the time series. If the sampling rate is high, resulting in a low reciprocal value of temporal resolution  $\Delta t$ , the time series and the derived self-consumption can be mapped with a high degree of detail.

Not surprisingly, a substantial number of studies [1-7] in the literature quantitatively investigate the impact of temporal resolution on self-consumption—mostly in a similar fashion. To begin, the reference value for self-consumption is established at the highest resolution ( $\Delta t_{\text{ori}}$ ). This resolution depends for example on the sampling rate of the measurement or on the best possible output of profile generators. Then the

quality of the time series is artificially degraded to a coarser resolution and the self-consumption is recalculated. The resulting deviation is expressed as a relative ratio, representing the error. Table 1 presents the outcomes of several studies, summarising the initial resolution with the resulting error when averaged on an hourly basis.

Table 1 Exemplary values from literature for the error of self-consumption when averaging from the original temporal resolution to 1 h

Reference	$\Delta t_{\text{ori}}$	Error
[1] Ried 2015	1 s	17–19 %
[2] Ayala 2018	10 s	9 %
[3] Beck 2016	10 s	3–20 %
[4] Stegner 2016	15 s	15–20 %
[5] Sun 2020*	15 s	14–38 %
[6] Jaszczur 2021**	1 min	6–14 %
[7] Jimenez 2021	1 min	5–15 %

\*Sun use the difference in %-points and only one reference value of 21 % is given. So, the 3–8 %-pt from the reference translate to the indicated relative error.

\*\*Jaszczur indicates values for selected single days only.

The literature unanimously agrees that the error in determining self-consumption rises as  $\Delta t$  increases. For detailed reasoning, please refer to the comprehensive explanation in [4]. Regardless of varying scenarios or specific conditions, the

following can be summarised based purely on the mathematical causes:

- The greater  $\Delta t$ , the greater the error
- The error is necessarily always positive.
- The error is higher when the time series are more volatile.
- If the time series are at a similar level, meaning there are numerous intervals with comparable power values of load and generation, the error escalates.

The last point is particularly relevant, because the optimisation goal when dimensioning a PV system is often to achieve the best possible balance between generation and load, i.e. the range more prone to error.

Even though battery coupled PV systems are not the subject of this study, another fact should be mentioned [3-5]:

- If an Electric Storage System (ESS) is used in combination with the PV system, the error in determining self-consumption is greatly reduced, even for high  $\Delta t$  of 1 h.

However, there is no contradiction but rather an almost similarly large underestimation of indirect self-consumption by the ESS added to the above-mentioned and still existing error of overestimating the direct self-consumption. Again, reference is made to [4], where the temporal averaging of the profiles is paraphrased with the existence of a virtual storage capacity, or, as [5] puts it: " In other words, the battery has a similar effect to simulating at low time resolution, but truly rather than erroneously."

This study is in line with the literature in Table 1 in terms of objectives and approach. However, it contains two innovations. Firstly, the mathematical background for the calculation of characteristic values of self-consumption is dealt with in detail and dependencies are formulated in the form of new functional equations. Secondly, the data used represent a quality in terms of the granularity and duration of the measurements that, to the author's knowledge, has not been achieved before. Above all, the use of measurement data collected from households, as well as a small takeaway restaurant and a mixed commercial area, presents a unique feature. This includes measurements with an extremely high temporal resolution of 1 s, that were carried out at three locations over a total period of more than one year.

## 2. Methodology

### 2.1. Data

One source of data was the measuring campaign described in [8]. Load and PV profiles with a  $\Delta t$  of 15 s were recorded by enhanced smart meters with high completeness for the year 2015. Data from this source will be referred to as *Smart Meter* data. Additional measurements were carried out within the InEs project (<https://ines-winterlingareal.de>) using different equipment, the Power-Energy Logger PEL103 from Chauvin Arnoux. This mobile instrument facilitates logging of voltage, current, power and energy values with a  $\Delta t$  of 1 s. It was temporarily used at three sites: at the Point of Common Coupling (PCC) of a mixed commercial site for 9 months, the

former porcelain factory that is the subject of the InEs project, at the PCC of a fast-food takeaway for 3 months, and at the PCC of a home with two occupants for 8 months. Data from this source will be referred to as *PEL* data. The PEL data does not include PV measurements and its load profiles are matched with PV profiles from the Smart Meter data. To give some more details on the mixed commercial profile: The occupancy of the InEs site may vary, usually accommodating 10 to 20 tenants. These may include various entities such as craft businesses like carpenters, small industries like metalworking companies, online retailers, as well as start-ups and small businesses in the technology sector. To the best of the author's knowledge, only [3] contains data of comparable quality concerning volume, such as the number and length of measurements, and temporal resolution.

### 2.2. Definition of self-consumption

When installing a PV system to meet the local electrical energy demand, the self-consumption is calculated by matching the time series of the generated PV power ( $P_{PV}$ ) with the time series of the power demand or load ( $P_{dem}$ ). These time series are considered as step functions with a constant temporal resolution ( $\Delta t$ ), consisting of  $N$  power values ( $P_i$ ) that are constant in each interval starting from and including  $t_i$ . The considered time window ( $T$ ) therefore has a duration of

$$T = N \times \Delta t \quad (1)$$

To calculate the overall Self-Consumption ( $E_{SC}$ ), which refers to the energy produced and consumed on site, the minimum value between the generation and the load must be determined for each interval separately.

$$E_{SC} = \sum_{i=1}^N \min(\{P_{PV,i}, P_{dem,i}\}) \times \Delta t \quad (2)$$

The PV yield  $E_{PV}$  for  $T$  is given by

$$E_{PV} = \sum_{i=1}^N E_{PV,i} = \sum_{i=1}^N P_{PV,i} \times \Delta t \quad (3)$$

The total electrical consumption ( $E_{dem}$ ) is calculated accordingly to (3) by integration of  $P_{dem,i}$ . Instead of the absolute value of  $E_{SC}$ , the Self-Consumption Ratio (SCR) and Self-Sufficiency Ratio (SSR) are often of interest because they enable comparing different setups and applications effectively. SCR is also known as the supply cover ratio, while for SSR, the terms load cover factor and autarky are often used. Both these values are calculated similarly, relating self-consumption to either the PV yield (in the case of SCR) or the total load (in the case of SSR):

$$SCR = E_{SC} / E_{PV} \quad (4)$$

$$SSR = E_{SC} / E_{dem} \quad (5)$$

### 2.3. Self-consumption formulated as function

SCR and SSR are the main protagonists of this study and are presented as a function of the main influencing variable, which is the size of the PV system—or a characteristic value derived

from it. However, there are other parameters that also have an impact:

- Location: climatic ambient conditions, seasonal variations
- Orientation of PV modules: azimuth and inclination
- Shape or complexity of the load time series: user behaviour, controllers, number and type of devices

This list is by no means exhaustive, but is intended to give you an idea of the scope.

The mathematical relationships between the characteristic values for self-consumption and functional dependencies will be explored in greater detail below. As previously stated, the size of a PV system is the most significant factor in real-world applications. However, using the installed PV module power to represent PV system size would require additional details of its positioning and orientation to draw conclusions regarding the power output. Instead, in order to increase comparability, it has proven useful to introduce an additional metric for the ratio of generated to required energy, the Prosumer Ratio (PR):

$$PR = E_{PV} / E_{dem} \quad (6)$$

With which (4) can be rewritten as

$$SCR = SSR / PR \quad (7)$$

A PR of 1 indicates a PV system that generates the exact amount of energy consumed during the time period T, regardless of the PV system's characteristics, which corresponds with the term Zero Energy Building (ZEB) used for example in [2]. This feature makes PR a good proxy to represent the size of a PV system. Additionally, the modular nature of a PV system justifies the use of PR as a linear scaling variable with respect to the output  $P_{PV}$ . It is therefore assumed, that if a PV system has a PR of 2, it will not only produce twice as much energy in T as an equivalent system having a PR of 1, but will also generate twice as much power during each interval i.

This results in the subsequent usage of PV time series in this investigation. Initially, a measured PV profile is proportionally adjusted to a PR of 1 with respect to the load profile considered, and the index PVE is used for such a PV system in Equilibrium with the load. As a consequence of the definition of PR,  $E_{PVE}$  is equal  $E_{dem}$ . The simulated PV power can then be expressed as

$$P_{PV} = PR \times P_{PVE} \quad (8)$$

As an aside, since this study uses the ratio between production and consumption (PR) as the function variable, scaling the load curve  $P_{dem}$  could also have been an option to achieve the desired effect. However, in our experience, linear scaling of load time series leads to unrealistic synthetic profiles. For example, a household with higher consumption will normally use appliances more often and for longer periods of time, but will not use twice as many appliances in parallel. We therefore prefer to leave the load time series as measured and scale the PV side, although it would not have made a difference in this study.

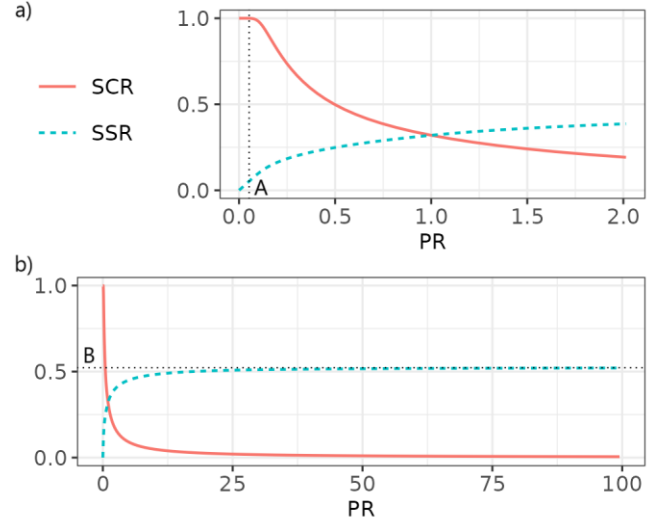


Figure 1 Exemplary curves for SCR and SSR as a function of the PV system size, indicated by the prosumer ratio  
 a) detailed view on low PR values  
 b) zoom out for trends toward infinity

Figure 1 illustrates two sample curves for SCR and SSR plotted against PR. Subfigure a) provides information on the typical shapes at lower PR values, while subfigure b) extends the x-axis to illustrate the behaviour towards infinity. Two dotted lines indicate values of particular interest. Point A on the x-axis marks the PR value where the SCR falls below 1 for the first time. As SSR is equal to PR multiplied by SCR, see (7), this makes point A the spot where SSR diverges from the origin line. The second line labelled with B on the y-axis marks the horizontal asymptote of SSR. Equation (7) confirms the obvious hyperbolic trend of SCR towards infinity as the curve approaches the function  $B/PR$  from the lower side.

#### 2.4. Analysing the stochastic background

The asymptotes A and B in figure 1 can easily be observed but their interpretation requires further investigation. Although  $P_{PVE}$  is scaled to ensure that its integral over T is equal to the corresponding integral of  $P_{dem}$ , it does not guarantee balanced power values in each interval. Instead, a Performance Ratio at overall Equilibrium ( $PRE_i$ ) can be calculated for each interval by

$$PRE_i = P_{PVE,i} / P_{dem,i} \quad (9)$$

$PRE_i$  will differ from 1, i.e. equilibrium, in most cases. Generation and consumption within an interval are deemed balanced if

$$PR \times PRE_i = 1 \quad (10)$$

Thus, point A on the x-axis marks the PR at which the first interval (that with the highest  $PRE_i$  ratio) reaches its equilibrium. We will refer to these PR values as the tipping points ( $TP_i$ ) of an interval i and, rewriting (10), they are defined as the reciprocal of  $PRE_i$

$$TP_i = 1 / PRE_i \quad (11)$$

Exceeding the tipping point results in a surplus of power ( $P_{SP,i}$ ) within this interval, which would typically be supplied to the grid or curtailed.

$$P_{SP,i} = P_{PV,i} - P_{dem,i} = (PR - TP_i) \times P_{PVE,i} \quad (12)$$

As PR increases, additional intervals steadily reach their tipping point and contribute to the surplus, thereby increasing the total surplus of energy ( $E_{SP}$ ) and influencing  $E_{SC}$

$$E_{SC} = E_{PV} - E_{SP} = E_{PV} - \sum \left( (PR - TP_i) \times E_{PVE,i} \right) \quad (13)$$

Please note that the sum in (13) only takes those intervals  $i$  into account, where the term  $PR - TP_i$  is positive, indicating that PR has passed the respective tipping point. To maintain better readability, there is no inclusion of a respective case distinction in equation (13). By incorporating equation (13) into equation (4), SCR can be reformulated as a function of PR:

$$\begin{aligned} SCR(PR) &= (E_{PV} - E_{SP})/E_{PV} = 1 - E_{SP}/(PR \times E_{PV}) \\ &= 1 - \sum \left( \frac{PR - TP_i}{PR} \times \frac{E_{PVE,i}}{E_{PVE}} \right) \end{aligned} \quad (14)$$

The first fraction following the sum symbol converges towards 1 for high PR values. The collective sum of the second fraction  $E_{PVE,i}/E_{PVE}$  for all intervals likewise amounts to 1, providing an explanation for the fundamental form of  $SCR(PR)$ : beginning at 1 and reducing to 0. To acquire a deeper comprehension regarding the contribution of each interval in equation (14), the term in the sum is presented visually in figure 2 as an example. It demonstrates that the corresponding function reaches zero when PR is equal to  $TP_i$ , possesses a vertical asymptote at  $PR = 0$ , and a horizontal asymptote at  $E_{PVE,i}/E_{PVE}$ . The slope of the function at  $TP_i$ , marking the initiation of its negative contribution to  $SCR(PR)$ , is  $E_{PVE,i}/(TP_i \times E_{PVE})$ .

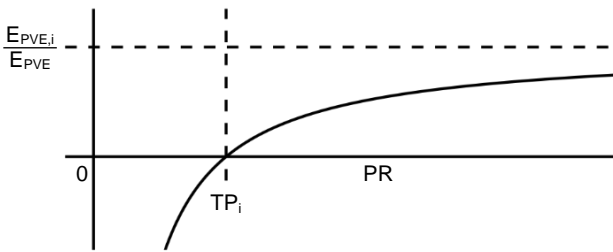


Figure 2 Schematic curve for the sum term in (14)

Thus, only the interpretation of the horizontal asymptote  $B$  of  $SSR$  remains, for which a value less than 1 is observed. At night, there will be intervals during which  $P_{PV}$  is zero. In these intervals, the PV system can never cover the load, despite the value of PR. However, in all other intervals where  $P_{PV}$  values are above zero, the PV generation will eventually suffice if PR is sufficiently high. Thus, the load can be split into a diurnal component  $E_{dem,diu}$  and a nocturnal one  $E_{dem,noct}$ . The horizontal asymptote  $B$  then represents the proportion of the load that can be supplied by PV

$$B = E_{dem,diu} / E_{dem} \quad (15)$$

For the sake of completeness, a rewriting of  $SSR(PR)$  similar to (14) is given without derivation

$$SSR(PR) = PR - \sum \frac{PR \times P_{PVE,i} \times \Delta t}{E_{PVE}} + \sum \frac{P_{dem,i} \times \Delta t}{E_{dem}} \quad (16)$$

Again, the calculation only considers intervals in the sums where PR exceeds  $TP_i$ . For high PR values the first sum becomes PR, eliminating the first term. The remaining second sum then corresponds to (15).

### 2.5. Sensitivity analysis regarding the temporal resolution

The determination of the error of the self-consumption in dependency of  $\Delta t$  will be conducted as outlined in the introduction. The following questions are to be examined.

1. Can recommendations be derived as to which temporal resolutions are necessary?
2. Is the temporal resolution of photovoltaics of secondary importance, as is often claimed, for example in [3, 5]?
3. How much does the aggregation of profiles reduce the error?

## 3. Results and discussion

### 3.1. Data plausibility check and processing

When using data of such high resolution as in this research, measurement gaps are nearly inevitable. In the Smart Meter data case, lengthier gaps are primarily due to mobile signal failures or limitations. We believe that shorter gaps, consisting of a few timestamps, are caused by brief overloads of the computing units installed or delays in writing to the SD card. After analysing the data, the rule was established to linearly interpolate gaps of up to seven missing readings to achieve more consistent time series. The number seven was chosen because it frequently occurs in the measurement data as a gap length and not with regards to mathematical or physical considerations. Incorporating this gap length in the correction procedure helps to attain a higher completeness level. With the PEL data, even a shorter interpolation would be sufficient as, in most cases, only single measured values are missing.

Regarding temporal aggregation, i.e. the deliberate reduction of resolution by averaging, there are two ways to handle measurement gaps that remain after the linear interpolation. In the more stringent approach, any missing value within the analysed interval results in an NA value. This would result in time series with a considerably reduced scope, given that during subsequent matching, i.e. the simultaneous observation of generation and load profiles, a singular missing value suffices for removing the entire interval from the balance. The resulting lower energy quantities would reduce the significance of the result. In the second version, NA values are ignored and already one measured value per interval triggers the calculation of a valid mean value. This variant is afflicted with a certain inaccuracy, but allows significantly more intervals to be taken into account. Unlike the stringent

approach, the total energies  $E_{PV}$  and  $E_{dem}$  can also rise here with increasing  $\Delta t$ , but the relative changes are significantly less than 1 % in the used data, with the exception of one PV system. For that reason, the second, less restrictive version is applied in this study.

### 3.2. Function analysis

As previously explained, the functions  $SSR(PR)$  and  $SCR(PR)$  can be easily described at both ends, for low PR values until reaching the first tipping point and towards infinity. However, describing the behaviour in between and fitting it with a proxy function is more challenging. Of the two,  $SCR$  is the more illustrative candidate, so equation (14) shall be considered. The shape of the curve from reaching the first tipping point until the last is defined by two aspects:

1. The frequency distribution of the tipping points, since they trigger whenever a new interval is included in the sum
2. The magnitude of the negative contribution of each interval to  $SCR(PR)$ , defined by  $E_{PVE,i}/E_{PVE}$

Regarding the first point, figure 3 depicts the tipping point probability density function for a specific load and PV combination. The histogram displays characteristics of a right skewed density function.

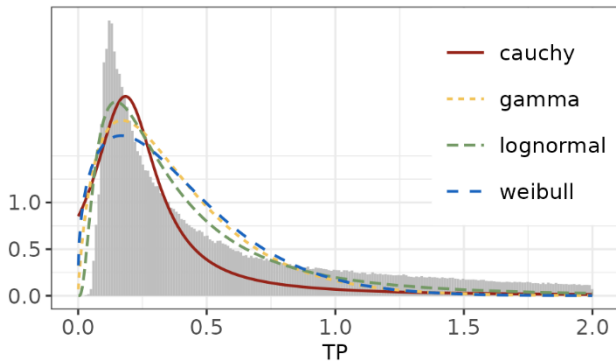


Figure 3 Tipping point density histogram as grey bins with fitted probability density function as different lines

Table 2 Results of the fitting of various distributions types to the histogram in figure 3

Distribution	1st param.	value	2nd param.	value
Cauchy	location	0.1839	scale	0.1489
Gamma	shape	1.7922	rate	4.6413
log-normal	meanlog	-1.1361	sdlog	0.8823
Weibull	shape	1.3791	scale	0.4280

When attempting to fit the histogram's shape using known asymmetrical distributions, such as Gamma, Cauchy, log-normal and Weibull, the log-normal distribution appears to be the most suitable. Cauchy comes close but approaches zero too quickly. Nevertheless, it should be noted that the histogram reaches high tipping point values far to the right. The further this range is considered when fitting, the less well the initial

peak at low tipping point values can be mapped. The resulting parameters for the fitted distribution functions are summarised in table 2.

The distribution of tipping points thus determines how quickly  $SCR$  and  $SSR$  approach the hyperbola  $B/PR$  and horizontal asymptote  $B$  respectively. With regard to dimensioning PV systems, individual, low tipping points are not advantageous, as they lead to high surpluses. Intervals with high tipping points are equally disadvantageous, as they can only be completely covered with large PV systems. Load management or shifting generation through differently oriented PV modules could help alleviate both phenomena. In a fictitious, ideal scenario, all tipping points would have identical values. This indicates that the shape of generation and load are perfectly matched, hence only the PV system needs to be adjusted in size. It should be noted that this common value of the tipping points would not be 1, but equal to  $B$ , as only  $E_{dem,diu}$  needs to be covered. The course of the corresponding  $SSR$  curve would follow exactly the origin line until the intersection with asymptote  $B$  is reached, thus revealing the value of  $PR$  that would be needed to reach maximum self-consumption with no surplus, namely also  $B$ .

The benefit of using established distributions is that they also define a cumulative distribution function. The trajectory of the  $SCR$  function from 1 to 0 resembles such a curve. However, the individual intervals do not contribute to the decrease of  $SCR$  with their frequency, i.e. the value 1, but with the term  $E_{PVE,i}/E_{PVE}$ , see also the second point above. This represents a kind of weighting of the intervals. Therefore, it is necessary to examine whether there exists a correlation between the value pairs of the tipping point and  $E_{PVE,i}/E_{PVE}$  or if they are stochastic, i.e. independent. Figure 4 reveals their corresponding 2D frequency distribution as a heat map, which demonstrates a distinct functional connection that resembles a hyperbola.

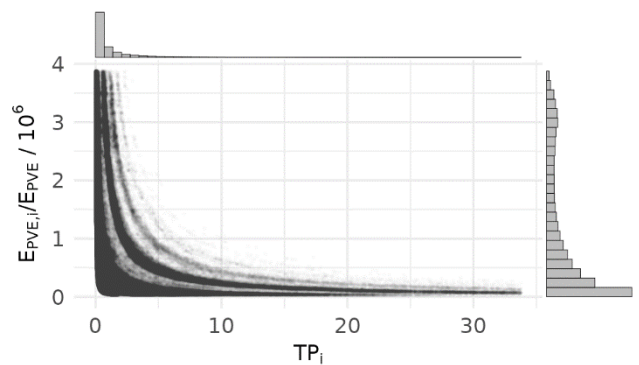


Figure 4 2D frequency distribution of the tipping points and the term  $E_{PVE,i}/E_{PVE}$  with additional histograms over each axis

The hyperbolic trend displayed in Figure 4 leads to high values of  $E_{PVE,i}/E_{PVE}$  at small tipping points. It should be recalled that the shape of the  $SCR$  curve arises from subtracting several curve segments, as illustrated in Figure 2, from the horizontal line at  $SCR = 1$ . Segments starting early at low PR are more frequent and contribute more significantly, as seen in Figure 4, thereby increasing the distribution's skewness.

3.3. Error of the self-consumption in dependency of  $\Delta t$

For the evaluation, the three loads from the PEL data and the seven residential loads from the Smart Meter data (labelled *load 1* to *load 7*) were individually matched with one of the seven PV profiles (also Smart Meter data). A further, aggregated load profile was created by accumulating the seven residential loads similar to [7], labelled *acc. Loads*. To also add the residential profile from the PEL data to the latter was not possible, as it does not cover a whole year yet and, since it stems from a different year, working days do not match. The study varied PR across a wide range and gradually increased the temporal resolution from  $\Delta t_{ori}$  to one hour, independently for the load and PV profiles. In this manner, around 180,000 permutations were simulated and, thanks to the high completeness, meaningful  $E_{SC}$  values were calculated—in the case of the PEL data over periods of different numbers of months, in the case of the Smart Meter data over one year each. The resulting values for SCR and SSR at  $\Delta t_{ori}$  are summarised in figure 5. It becomes apparent that for SSR the respective height of B does not necessarily correlate with the speed at which the curve approaches the asymptote, an outlier being the fast-food takeaway. One possible explanation for this is that because of the non-operating days with low base load, surplus is already generated at low PR, but the remaining load on weekdays and Saturdays correlates very well with generation, resulting in the maximal horizontal asymptote of its SSR(PR).

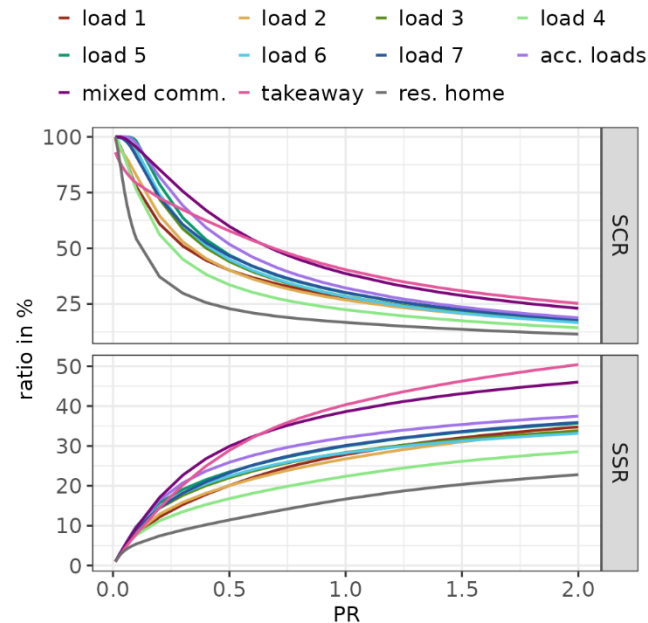


Figure 5 Ratios of self-consumption against different PV sizes

The self-consumption error was computed as the difference between  $E_{SC}$  and the corresponding reference value at the original resolutions, divided by that same reference value. Regardless of whether SCR or SSR were used instead of  $E_{SC}$ , the resulting relative error is identical. The selection of the PV profile has negligible impact on the outcomes. Therefore, this paper solely focuses on the combinations with one PV system, specifically the measurement with the highest degree of completeness. Figures 6 and 7 summarise the results for the Smart Meter and the PEL load profiles respectively.

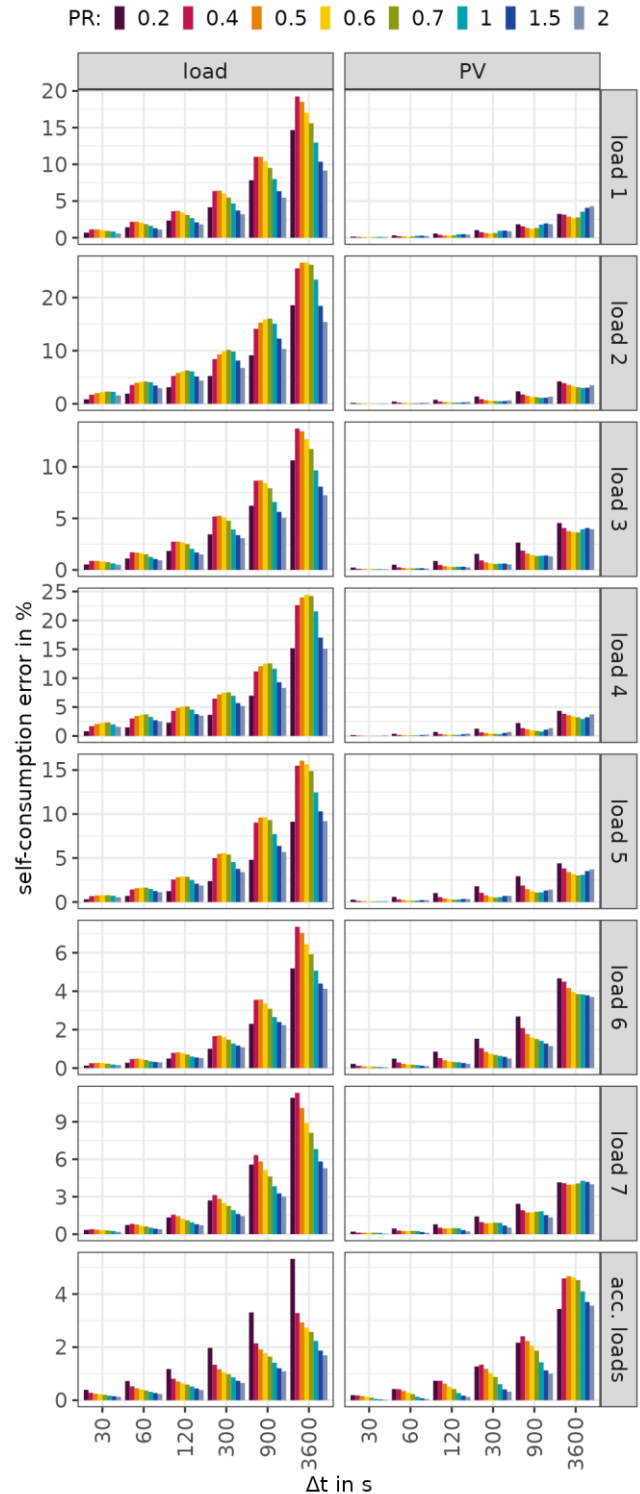


Figure 6 Resulting error in the calculated self-consumption when the temporal resolution of the load (left column) and the PV (right column) is degraded for the seven residential Smart Meter loads and their accumulated profile

The following main findings can be observed:

- The relative error peaks at PR values of 0.4–0.6 when varying the load’s temporal resolution.
- In case of varying  $\Delta t$  of the PV there are two trends: For the loads with higher demand (mixed commercial site, fast

food takeaway and the accumulated households) the peak shifts to higher PR values of 0.5–1. For individual residential profiles the error rises towards the two extrema of PR to the left and right.

- The load’s temporal resolution has a higher impact on the increase of the error than the PV with exception of two scenarios: the mixed commercial site and the accumulated households.
- Accumulated loads like that of the seven residential profiles or the mixed commercial site exhibit lower error values.

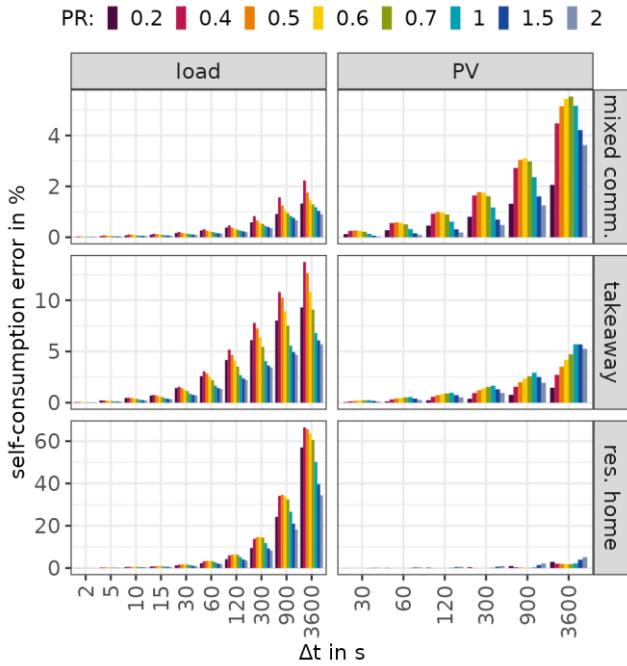


Figure 7 Resulting error in the calculated self-consumption when the temporal resolution of the load (left column) and the PV (right column) is degraded for the three PEL data locations

Three questions were outlined in section 2.5. and their investigation is summarised as follows. The PEL data falls short of the Smart Meter data in terms of their scope, specifically the number and duration of measurements. However, PEL were used not only in the residential sector but also in the commercial sector, including a fast-food takeaway and a mixed commercial area. The respective energy consumptions are ca. 65 kWh and 1.000 kWh on a weekday for the takeaway and the mixed commercial site of project InEs. On Sundays and public holidays they are much lower at 8 kWh and 400 kWh each. Additionally, the PEL data provides better temporal resolutions than the Smart Meters’ 15 s recordings. In order to provide a recommendation on the necessary temporal resolution, the PEL data are therefore particularly suitable due to their  $\Delta t$  of 1 s and the cross-sectoral use cases. A limit of 3 % is chosen as the acceptable error threshold. Figures 6 and 7 illustrate that a single, temporal minimum resolution cannot be derived. Instead, deviations are heavily influenced by the load profile’s character and the PR value. To answer question 1, PR is set as 1 as this ratio is a practical and standard dimension for real-world applications. Figure 8 illustrates the acceptable error threshold of 3 % using

a capped y-axis. Additionally, it provides information about the simultaneous degradation of both profiles’ resolution. Some scenarios already exceed the acceptable error limit at a  $\Delta t$  of 1 min, while almost all do so at 15 min.

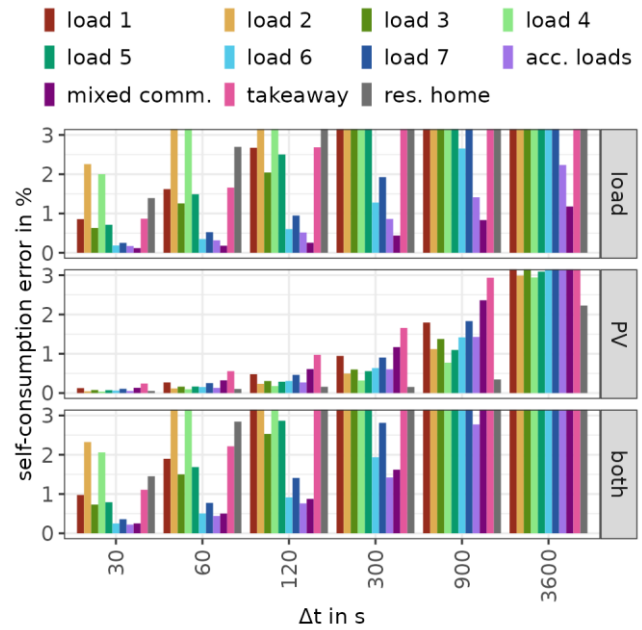


Figure 8 Condensed results with PR = 1 and limited y-axis

In relation to question 2, the effect of the load’s temporal resolution seems to be generally greater. However, due to opposing outcomes observed for the cumulative profiles, a definitive conclusion cannot be reached. Regarding question 3, it was previously noted that accumulating loads decreases the error. For the two such profiles in this study, even a  $\Delta t$  of 15 min would remain within acceptable limits.

#### 4. Conclusion and outlook

This study adds to the existing research on the influence of the temporal resolution on the PV self-consumption with two significant contributions. Firstly, a comprehensive analysis of the mathematical fundamentals is conducted. The obtained insights are valid irrespective of scenario-specific conditions and are relevant wherever time series of generation are matched with those of load. Thus, the dissection of the SCR and SSR function into intervals and the analysis of the stochastic influence are transferable to the use of other sources of energy too.

Secondly, the self-consumption of PV electricity is calculated under various scenarios. The evaluation extends the bandwidth compared to current literature by including the commercial sector in addition to residential loads and measurements with a temporal resolution as low as 1 s. The results thus provide a comprehensive and realistic insight into the expected ratios for self-consumption. The potential errors of coarser temporal resolutions are also analysed. The results exhibit a wide range, and further investigation is required to determine the factors that affect it, such as PV module orientation, total consumption and load profile characteristics. Especially for the

categorisation of load profiles with regard to their characteristics, there is a great need for research. A valuable overview of methods is provided in [9] and great potential is seen in the so called complexity measures introduced there, an assumption the author of the presented study endorses.

## 5. Acknowledgements

The research of this study was funded by the German Federal Ministry for Economics and Climate Action (BMWK) as part of the project EnEff:Stadt InEs.

## 6. References

### Journal articles

- [2] A. Ayala-Gilardón, M. Sidrach-de-Cardona, and L. Mora-López, ‘Influence of time resolution in the estimation of self-consumption and self-sufficiency of photovoltaic facilities’, *Applied Energy*, vol. 229, pp. 990–997, Nov. 2018, doi: 10.1016/j.apenergy.2018.08.072.
- [3] T. Beck, H. Kondziella, G. Huard et al., ‘Assessing the influence of the temporal resolution of electrical load and PV generation profiles on self-consumption and sizing of PV-battery systems’, *Applied Energy*, vol. 173, pp. 331–342, Jul. 2016, doi: 10.1016/j.apenergy.2016.04.050.
- [5] S. I. Sun, B. D. Smith, R. G. A. Wills et al., ‘Effects of time resolution on finances and self-consumption when modeling domestic PV-battery systems’, *Energy Reports*, vol. 6, pp. 157–165, May 2020, doi: 10.1016/j.egy.2020.03.020.

- [6] M. Jaszczur, Q. Hassan, A. M. Abdulateef et al., ‘Assessing the temporal load resolution effect on the photovoltaic energy flows and self-consumption’, *Renewable Energy*, vol. 169, pp. 1077–1090, May 2021, doi: 10.1016/j.renene.2021.01.076.
- [7] G. Jiménez-Castillo, C. Rus-Casas, G. M. Tina et al., ‘Effects of smart meter time resolution when analyzing photovoltaic self-consumption system on a daily and annual basis’, *Renewable Energy*, vol. 164, pp. 889–896, Feb. 2021, doi: 10.1016/j.renene.2020.09.096.
- [8] C. Stegner, O. Glaß, and T. Beikircher, ‘Comparing smart metered, residential power demand with standard load profiles’, *Sustainable Energy, Grids and Networks*, p. 100248, Sep. 2019, doi: 10.1016/j.segan.2019.100248.
- [9] S. Köhler, R. Rongstock, M. Hein et al., ‘Similarity measures and comparison methods for residential electricity load profiles’, *Energy and Buildings*, vol. 271, p. 112327, Sep. 2022, doi: 10.1016/j.enbuild.2022.112327.

### Conference Paper

- [1] S. Ried, P. Jochem, and W. Fichtner, ‘Profitability of photovoltaic battery systems considering temporal resolution’, in *2015 12th International Conference on the European Energy Market (EEM)*, IEEE, 2015, pp. 1–5.
- [4] C. Stegner, J. Bogenrieder, P. Luchscheider et al., ‘First year of smart metering with high time resolution—realistic self-sufficiency rates for households with solar batteries’, presented at the *IRES 2016*, Mar. 2016.